4B.1 **Towards Completing the Rain Drop Size Distribution Spectrum:
A Case Study Involving 2D Video Disdrometer, Droplet Spectrometer, and
Polarimetric Radar Measurements in Greeley, Colorado**

M. Thurai[1], V. N. Bringi[1], P. C. Kennedy[1], B. Notaros[1], and P. N. Gatlin[2]
[1]Colorado State Univ., Fort Collins, CO
[2]NASA/MSFC, Huntsville, Alabama

1. Introduction

Rain drop size distribution (DSD) measurements have been made over the past several decades with many different types of instruments and in many different locations. Of all the instruments, the 2D video disdrometer (2DVD; Shönhuber et al., 2008) has been established as the most suitable instrument for measuring the large drop end of the DSD spectrum (Gatlin et al., 2015). On the other hand, this instrument does not reliably measure the drop concentration for drop diameters less than 0.7 mm; in fact, it tends to underestimate N(D) for these small drops. The problem is related to lowered sensitivity to small and tiny drops, the associated difficulty in matching of these drops from the two camera images and to finite instrument resolution.

In an attempt to achieve a complete drop size distribution in rain, in April 2015, a droplet spectrometer (Meteorological Particle Spectrometer, MPS) was installed next to a 2DVD at a site near Greeley, Colorado. Both instruments were conveniently installed within a 2/3-scaled DFIR double wind-fence, located at about 13 km from the CSU-CHILL S-band polarimetric radar. Inside the DFIR, there were several other instruments including a Pluvio weighing bucket-type raingauge.

Since the MPS installation, many events have been recorded by all three ground instruments, and for several of these events, the CHILL radar scans were made at regular and closely spaced time intervals comprising VAD, sector, PPI and RHI scans. Table 1 summarizes the main events recorded from mid-April to mid-June of 2015. During this period, the Greeley area had unusually high rainfall, and this can also be seen from Table 1. Note that from mid-May 2015, dual-frequency CHILL measurements were made at S and X band.

Table 1: Major rain events recorded (mid Apr – mid June 2015)

Date	24 hour Rain accum, mm
17 Apr	17.1 (*)
26 Apr	12.9
03 May	7.3
06 May	24.7 (*)
08 May	30.6 (*)
09 May	21.5
10 May	Melting snow
19 May	37.1
22 May	6.7 (**)
23 May	10.1 (**)
24 May	1.8
29 May	8.3 (**)
30 May	1.5
01 Jun	1.4
05 Jun	rain-hail mixture (**)
11 Jun	0.4 (**)
14 Jun	0.27
16 Jun	1.9 (**)

(*) indicates CHILL S-band observations
(**) indicates CHILL S and X band data
Note: the event on 05 June is referred to in Manic, et al., 2015.

In this paper, we consider one event which occurred very soon after the MPS

installation (17 April 2015), a long-duration but intermittent rain event which was part of a mid-latitude synoptic scale cyclone that had produced fine drizzle, light precipitation, cold rain, rain bands, both stratiform and convective in nature, as well as thunderstorms towards the end of the event. We present here a near-complete picture of the DSD spectra (from tiny to large drops) by combining the MPS and 2DVD measurements for the different variety of rain-types, and correlate the main DSD parameters (such as the mass-weighted mean diameter) with the S-band CHILL data.

2.   Instrumentation

2.1:   MPS, 2DVD and Pluvio

Fig. 1 shows the three instruments installed within the double wind fence. In all three cases, the sensor area was set at the recommended height relative to height of the inner fence.

Fig. 1: The MPS, 2DVD and Pluvio inside the double wind fence, and the newly installed POSS.

The MPS uses a linear array of 64 photodiodes to measure the shadow images of particles falling through a collimated laser beam. The concepts of the technique were originally introduced by Knollenberg (1970). This instrument has 50 micron resolution and is suitable for measuring small and tiny drops. It's size range is 50 microns to 3.1 mm and its sampling area is 6.2 cm^2. The 2DVD

on the other hand has a much larger 10 by 10 cm^2 sensor area (Schönhuber, et al., 2008) but the pixel resolution for the front and side view (silhouettes) is around 170 microns.

Whilst the MPS enabled drop concentration measurements down to 0.1 mm, the 2DVD had recorded drops as large as 5 mm associated with the (non-hail producing) thunderstorm for the 17 April event. Fall velocities show a clear trend with drop diameter, in agreement with the expected Gunn-Kinzer variation, but with an adjustment factor appropriate for the 1.4 km altitude for Greeley (see Fig. 2). Further, shape information also confirmed that almost all the hydrometeors were rain drops.
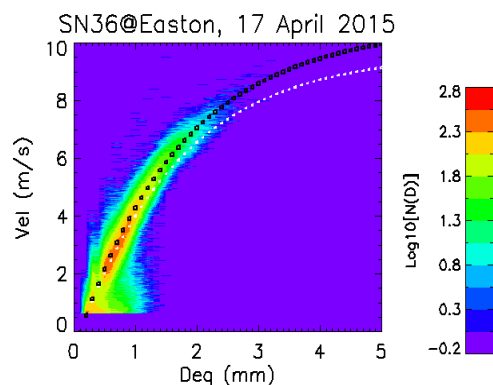
Fig. 2: Fall velocity versus drop equi-volume diameter, D_{eq} from the 2DVD data as 2D frequency of occurrence plot. The white dotted line represents the equation given in Atlas et al. (1973) and the black dotted line is derived after applying altitude correction for the 1.4 km a.s.l. for Greeley.

The Pluvio we used is the 2nd generation weighing type rain gauge manufactured by OTT with a 200 cm^2 collection area that utilizes a highly precise load-cell to enable study of rainfall amounts as little as 0.1 mm with an accuracy of 0.2% (OTT Messtechinik GmbH 2010).

2.2   CSU_CHILL radar

The CSU-CHILL radar is an S-band research-grade, polarimatric weather radar, operated by Colorado State University. One of the main features of this system is the 8.5 m dual-offset Gregorian antenna with particularly high cross-polar performance at S-band (Bringi et al., 2011). During this current campaign, a dual wavelength feedhorn was installed (mid May 2015), however, for the event presented here, i.e. 17

April 2015, only the S-band system was utilized.

The S-band LDR from 10 degree elevation VAD scans showed extraordinarily clear 'melting layer circles' at times. One example is given in Fig. 3. The clarity of the melting layer circle was far better than those obtained from Z_{dr} or ρ_{hv}, mainly because of the high cross-polar performance of the custom-made antenna design.
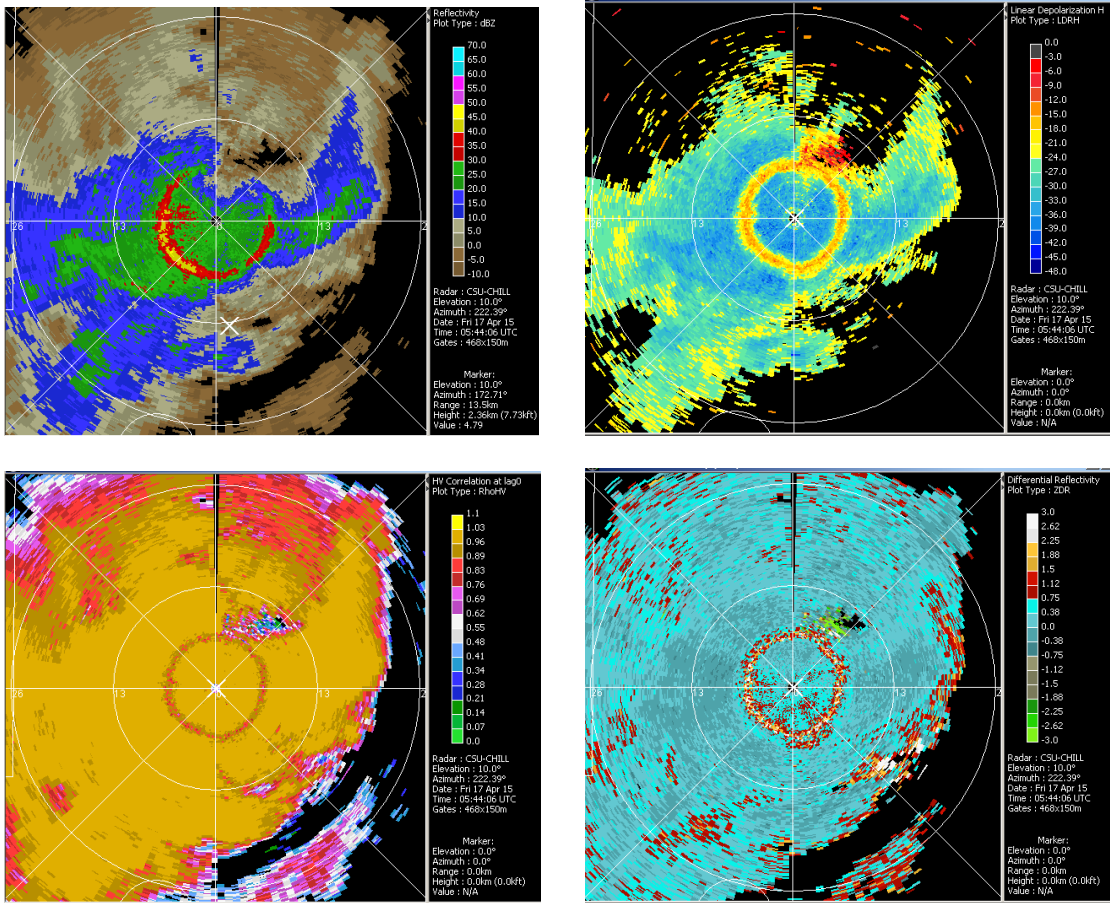
Fig. 3: CHILL S-band dBZ (top left) and LDR (top right), ρ_{hv} (bottom left) and Z_{dr} (bottom right) from a 10 deg VAD scan made at 19:48 UTC on 17 April 2015. LDR shows the clearest melting layer ring, both the 'innermost' region of the bright band as well as the top region and the bottom.

3.   17 April event analysis: DSD

As mentioned earlier, this event was an intermittent but long duration event which produced a variety of rain types. Fig. 4(a) shows the 1-minute rainfall rates (with running average over 3 minutes) from the 2DVD, and Pluvio measurements. Also shown is the combined 2DVD and MPS drop size distribution based rain rates (described later). Fig. 4(b) shows the corresponding rain accumulation comparisons for every 2 hours.

For drop size distribution comparisons between the 2DVD and MPS, we split the entire time series event into the same 2-hour periods as in Fig. 4(b), starting with 00:00 UTC and ending with 20:00 UTC. Fig. 5 shows these 2-hourly DSD comparisons, except for the first two hours and the last two hours. As seen, the agreement is reasonably close in the 0.7 to 1.2 mm drop diameter range. The 2DVD underestimates the drop concentration for smaller drops (as expected) compared with the MPS. For larger drops on the other hand the 2DVD measurements can be considered to be much more accurate than the MPS (which needs to make drop shape assumptions in order to compute the drop diameter).

Fig. 6(a) compares the mass-weighted mean diameters (D_m) calculated using the 2DVD DSD alone versus those using the 2DVD DSD modified with the MPS DSD for drop diameters < 0.7 mm. In both cases, D_m was calculated using 1-minute DSDs but averaged over three minutes. Compared with the [1:1] line, the bias is evident, and in almost all cases, the 2DVD based values tend to overestimate D_m, which is to be expected, but the

overestimation is higher when D_m < 1 mm, i.e. for DSDs where small drops play a more dominant role. The corresponding effect on the 1-minute R can be seen in Fig. 6(b). The effect of including the small drops from the MPS, as expected, increases R, and the effect is more noticeable for low R, particularly below 1 mm/h and even more so below 0.1 mm/h.

D_m histograms for three of the 2-hourly periods are compared/shown in Fig. 7. In each case, the predominant rain type is specified. Note the following:

(i)   For the light rain case, the MPS-2DVD combined DSDs produce significantly lower D_m (histograms) than those from the 2DVD alone.
(ii) Convective rain produces similar D_m histograms.
(iii) During the thunderstorm period, the two histograms are similar, except at the lower end of the distribution.
(iv) The MPS-2DVD combined DSDs show D_m values lower than 0.5 mm for light rain.

D_m histograms were also compared for various 1-minute rain rate intervals. Fig 8 shows these comparisons for the whole event (02:00-20:00 UTC) for R<0.5 mm/h, 0.5<R<1 mm/h, and 1<R<5 mm/h. The trend in the differences in the D_m histograms is clear, that is, for low rainfall rates, the combined MPS-2DVD DSDs show significantly lower Dm values than those derived from the 2DVD DSDs alone, whereas for the higher rainfall rates there is no noticeable change. Hence the concentration of small drops has more impact on D_m for lower rainfall rates.
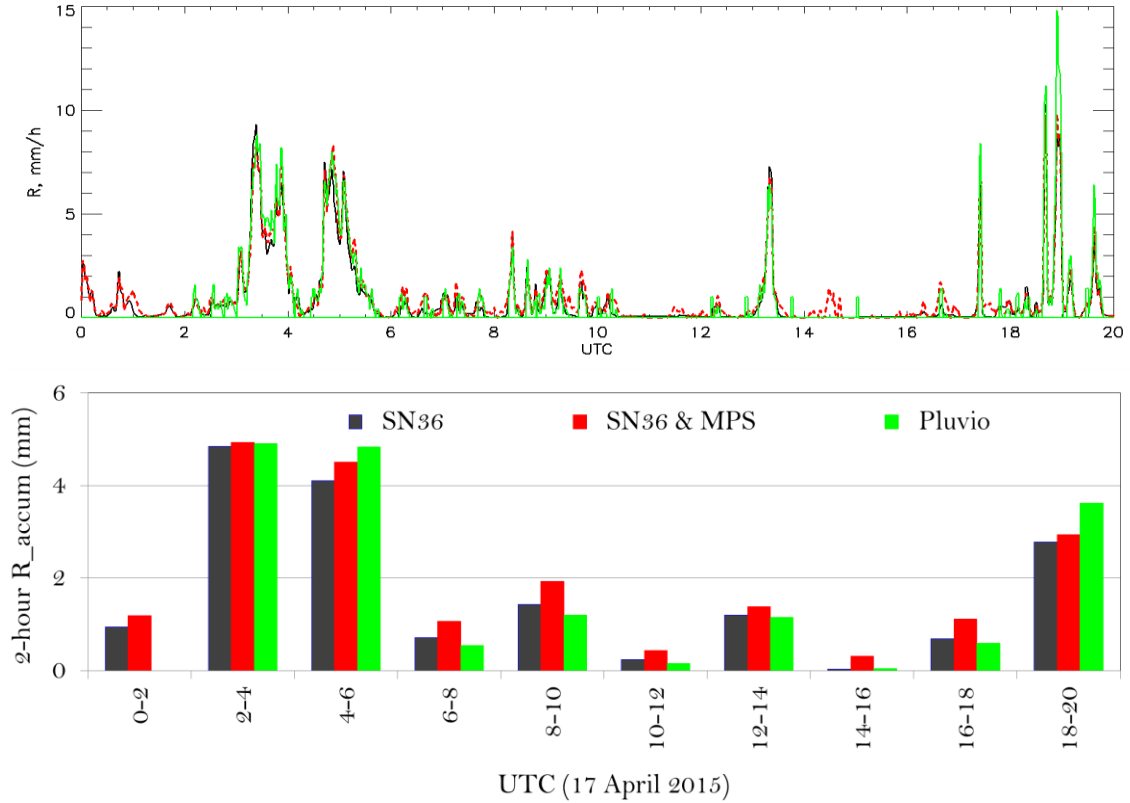
Fig. 4: *Top panel*: 1-minute rain-rate (R), averaged over 3-min, from 2DVD (black), Pluvio (green) and 2DVD-MPS combined drop size distribution-based estimates (red). *Bottom panel*: The corresponding 2-hour rain accumulations.
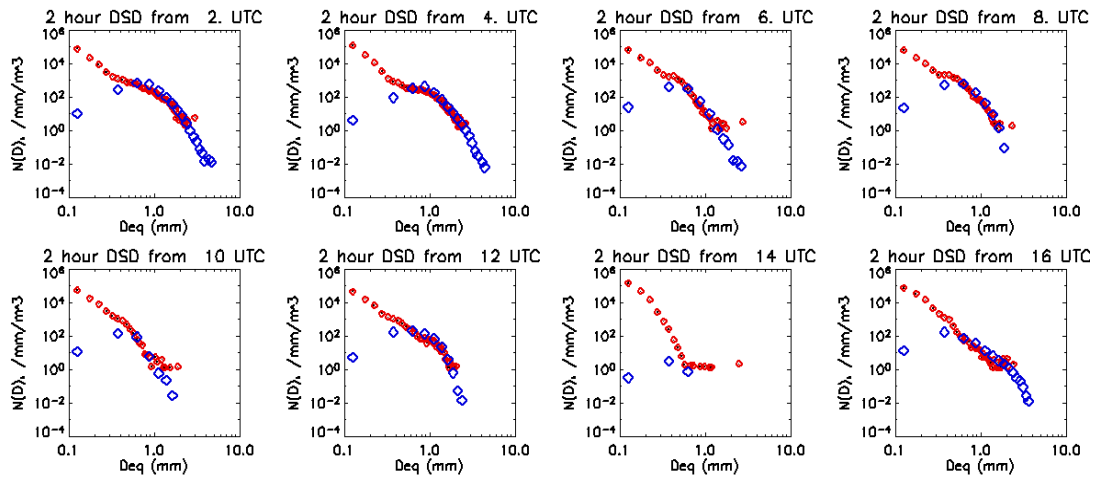
Fig. 5: 2-hour DSD comparisons from the 2DVD (blue) and 2DVD-MPS combined (red) for the 17 April event. The time interval is specified for each case.
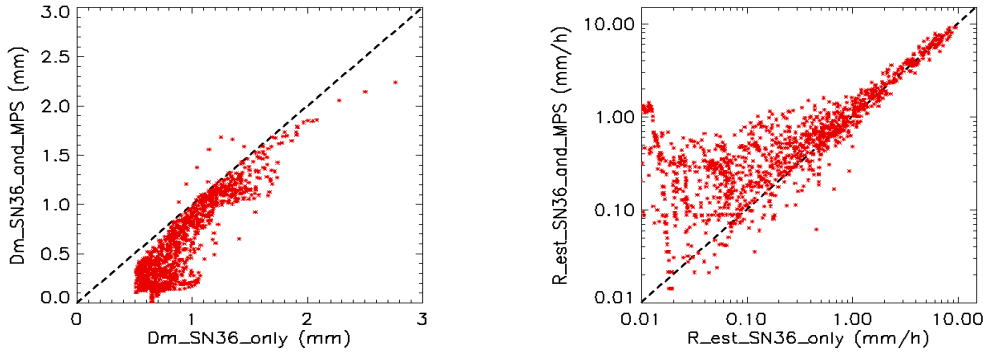
Fig. 6: : D_m comparisons between 2DVD-based and 2DVD-MPS combined DSD based estimates (left) and the corresponding R estimates (right).
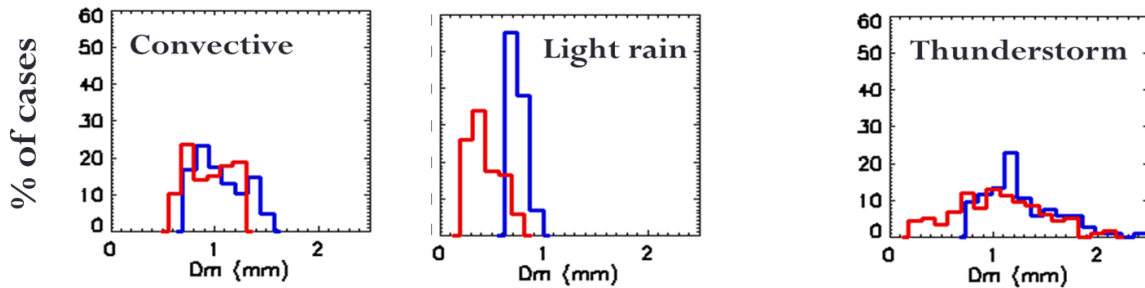
Fig. 7: D_m histogram comparisons between 2DVD-based and 2DVD-MPS combined DSD based estimates (blue and red respectively) for three 2-hour time intervals, namely, 0200-0400 UTC, 0800-1000 UTC, and 1800-2000 UTC. The predominant rain type is specified for each case.
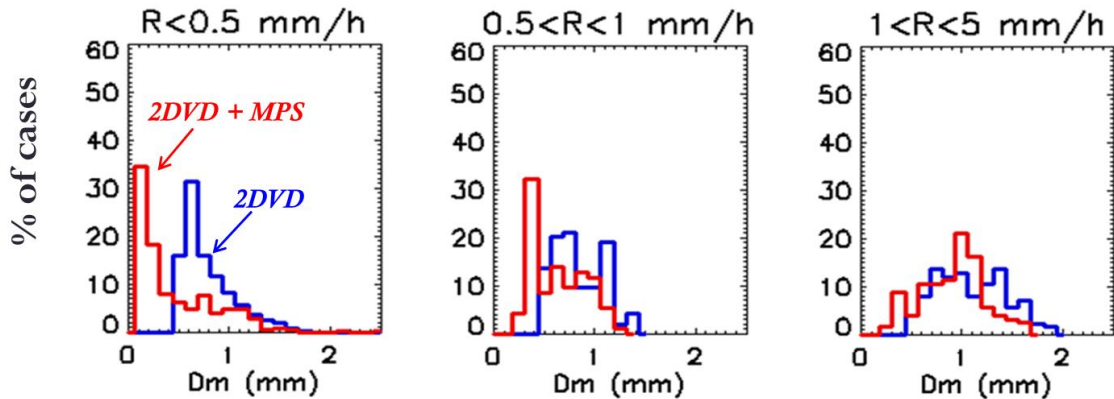
Fig. 8: D_m histogram comparisons between 2DVD-based and 2DVD-MPS combined DSD based estimates (blue and red respectively) for the various intervals.

4. Radar observations and analysis

As mentioned earlier, the CHILL radar scans were made at regular and closely spaced time intervals comprising VAD, sector, PPI and RHI scans. From the PPI and sector scans, the range profiles over the 2DVD/MPS/Pluvio site were extracted (az: 171.5 deg). The top two panels of Fig. 9 show the S-band Z_h and Z_{dr} range profiles as time series, and the next two panels show Z_h and Z_{dr} (red) extracted at ~ 13 km range, i.e. location of the instruments. These are compared with scattering simulations using the 1-minute DSD data at ground level (blue).

During the thunderstorm period (towards the end of the event), rapid fluctuation in Z_h (and R from Fig. 4 top panel) is noticeable whilst at the beginning (00:00 – 01:00 UTC) differences in measured Z_{dr} and calculated Z_{dr} (assuming rain) are noticeable which can be attributed to the presence of non-fully-melted snow during that time period. Other than these, the agreement in Z_h and Z_{dr} are close.

As mentioned earlier, and as specified in Fig. 7, a broad rain-type classification for each of the 2-hour period based on all the radar scans was made, as follows:

00-02 : melting snow, cold rain
02-04:moderate convective rain
04-06:moderate convective rain
06-08: drizzle
08-10: light rain
10-12: fine drizzle
12-14: mostly stratiform rain
14-16: fine drizzle
16-18: mostly stratiform rain
18-20: moderate thunderstorm

The last panel in Fig. 9 shows the time series of D_m determined from the .2DVD-MPS combined 1-minute DSDs, smoothed over 3 minutes. These

D_m's appear to be better correlated with S-band CHILL Z_h than with CHILL Z_{dr}, (which is somewhat surprising, even at S-band). Fig. 10 shows this more clearly which shows the variation of D_m from the 1-minute DSDs (again smoothed over 3-minutes) with the S-band Z_h and Z_{dr}. The blue points represent the D_m values obtained from the 2DVD data alone whilst the red points represent those derived from the 2DVD-MPS combined/composite DSDs. Because of the large spread in D_m for any given Z_h or Z_{dr}, it would seem more appropriate to use both parameters to determine D_m to a better accuracy. To this end, we have attempted to derive a fitted equation, given by $D_m^{est} = f(Z_h, Z_{dr})$.

The best fitted function for all the data was found to be:

$$D_m{}^{est} = 0.3607 \left(Z_{h\_lin}{}^{0.1595}\right) \left(Z_{dr\_lin}{}^{0.7683}\right) \quad (1)$$

where 'lin' indicates linear units. Values of estimated D_m from the above equation are compared with the measured D_m in Fig. 11 (black points). Reasonable agreement with [1:1] line is seen, but it should be noted that the above equation is only a preliminary fit and needs to be validated and/or improved for other rain events.

Referring back to Fig. 10 it is also worth noting that the D_m derived from the combined DSDs give rise to significantly different (lower) variations with CHILL Z_h and Z_{dr}, particularly for low Z_{dr} (Z_{dr} < 0.25 dB are denoted by filled red points in the lower panel). The fitted equation was derived for all Z_h and Z_{dr} values given for the entire event, using all the points in the bottom three panels of Fig. 9. Better fit/s can probably be derived for by thresholding Z_{dr}. This will be attempted in the future.
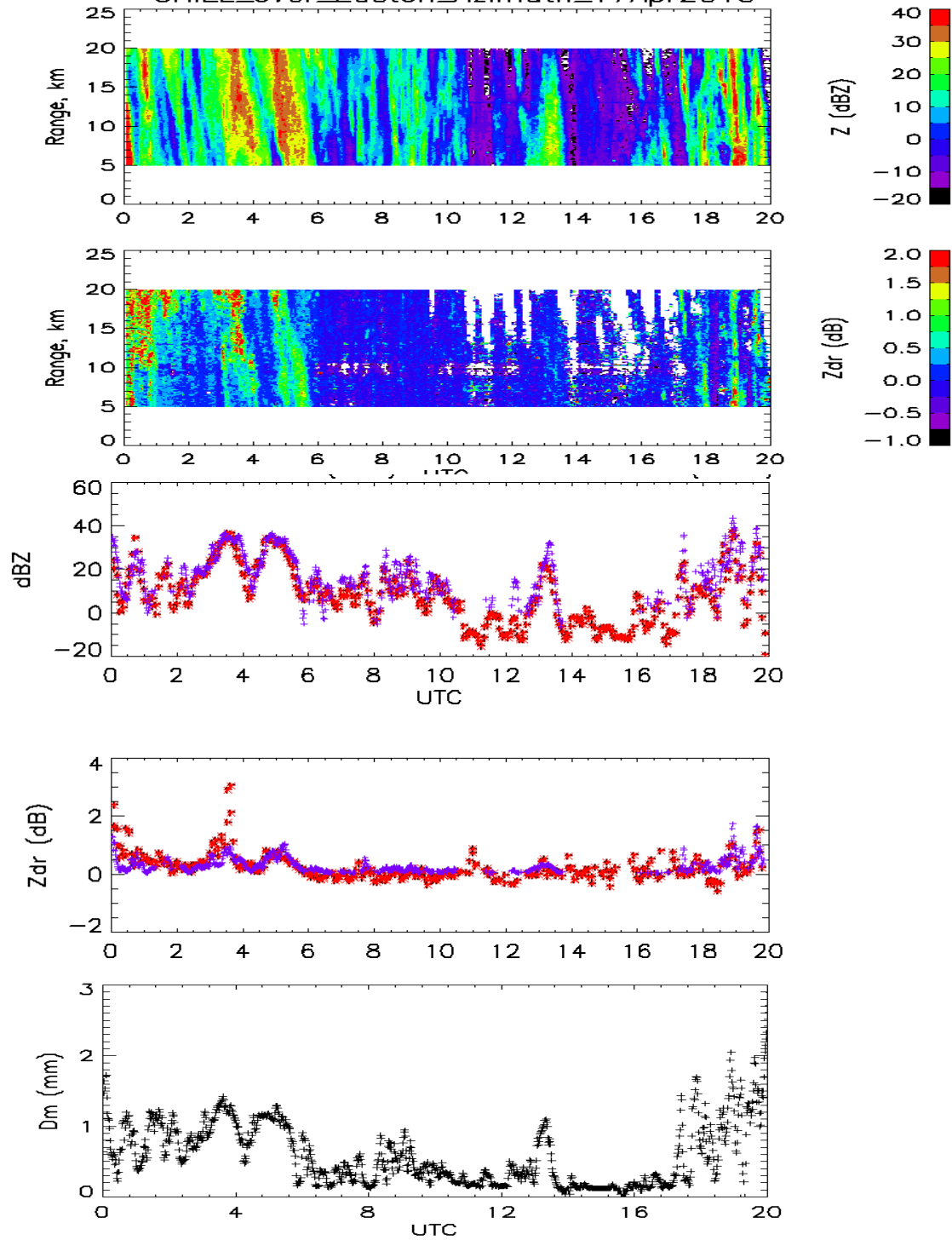
Fig. 9: Top two panels: range profiles of Z_h and Z_{dr} extracted from the CHILL S-band scans over the instrument site; next two panels: Z_h and Z_{dr} extracted from the CHILL S-band scans at and near the instrument site (red) compared with the 1-minute measured DSD (MPS-2DVD composite) based calculations (blue); last panel: D_m calculated from the 1-minute composite DSDs.
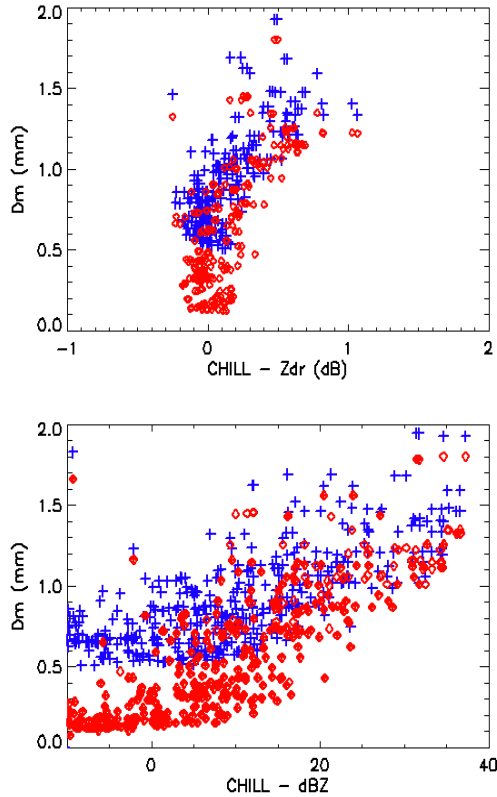
Fig. 10: D_m calculated using 2DVD (blue) and 2DVD-MPS combined 1-minute DSDs (red) versus the S-band measurements over the instrument site.
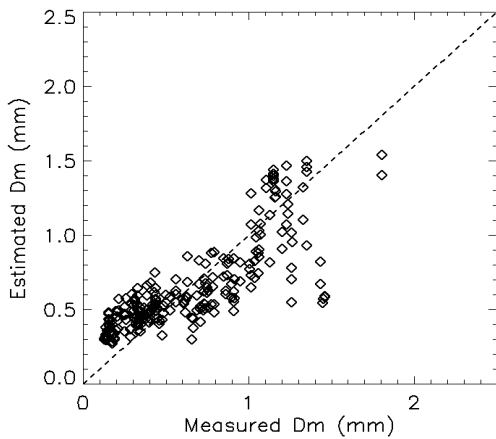
Fig. 11: Estimated D_m values from CHILL Z_h and Z_{dr} versus the measured D_m derived from the 1-minute combined DSDS. The black points represent those estimated using eq. (1) and the green points those using eq. (2).

Finally, in Fig. 12, we compare the standard deviation of the mass spectrum (σ_M) from the 1-minute DSDs 2DVD alone (red) and 2DVD-MPS combined (blue). For both cases, σ_M increases during the thunderstorm period (18:00 - 20:00 UTC) indicating wider DSDs, however, the combined DSDs result in noticeably higher σ_M. This change, together with the change in D_m values (as seen in Fig. 7, 8 etc.) may give rise to a somewhat modified σ_M–D_m relationship than those using the 2DVD data alone (Williams et al. 2014).
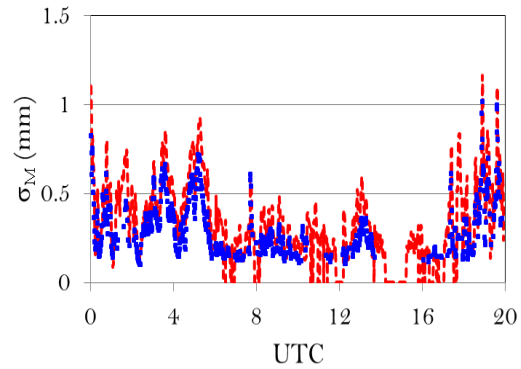
Fig. 12: Comparing 2DVD-based (blue) and 2DVD-MPS combined DSD-based (red) σ_M as time series for the event.

8   Summary

The combined DSDs derived from the collocated 2DVD and MPS measurements from the 17 April 2015 event have enabled us to improve the estimation procedures for the DSD parameters. Simultaneous scans from the S-band CHILL radar have provided a great opportunity to develop DSD retrieval algorithms for the S-band polarimetric radar measurements.

Table 1 has shown all the events recorded during the first two months of the 2015 rain-hail project in Greeley, Colorado. Since then, there have been several more events, including a microburst event in July 2015, have been recorded (see Thurai and Kennedy, 2015). From June 2015, X-band dual-polarization radar measurements have also been made (after the reinstallation of the dual wavelength feedhorn). Additionally, a precipitation occurrence sensor system (POSS) has been installed at the 2DVD-MPS site. The combined 2DVD-MPS-POSS-Pluvio data, together with the CSU-CHILL S- and X- band dual polarization measurements are providing unique datasets to Investigate rain drop shapes, size, and fall velocities as well as to conduct hail size, shapes and fall velocity investigations.

References

Bringi, et al., 2011: Design and Performance Characteristics of the New 8.5-m Dual-Offset Gregorian Antenna for the CSU–CHILL Radar. J. Atmos. Oceanic Technol., 28, 907–920.

Gatlin et al., 2015, Searching for Large Raindrops: A Global Summary of Two-Dimensional Video Disdrometer Observations. J. Appl. Meteor. Climatol., 54, 1069–1089.

Knollenberg, R.G., 1970: The optical array: An alternative to scattering and extinction for airborne particle size determination, J. Appl. Met., 9, 86-103.

S. Manic, E. Chobanyan, M. Thurai, V. N. Bringi, and B. M. Notaroš, 2015, Comparison of Simulated Scattering Characteristics of Large Rain Drops and a Special Form of Melting Hail and Relation to C, S and X Band Radar Observations, this conference (2015 AMS 37th Conference on Radar Meteorology, Norman, OK, Sept. 2015), poster paper 82, extended abstract.

OTT Messtechnik GmbH, 2010: Operating instructions Precipitation Gauge OTT Pluvio.]

Shönhuber et al., 2008, The 2D-video-vistrometer, Chapter 1 in "Precipitation: Advances in Measurement, Estimation and Prediction", Michaelides, Silas. (Ed.), Springer, ISBN: 978-3-540-77654-3, 2008.

Thurai M., and P. C. Kennedy, 2015, DPWX/Microburst winds and melting hail at the Easton Airport field site: 9 July 2015, See webpage: http://www.chill.colostate.edu/w/DPWX/ Microburst_winds_and_melting_hail_at_ the_Easton_Airport_field_site:_9_July_2 015

Williams, C.R., and Coauthors, 2014: Describing the Shape of Raindrop Size Distributions Using Uncorrelated Raindrop Mass Spectrum Parameters. *J. Appl. Meteor. Climatol.*, **53**, 1282–1296.